Journal of Clinical and Translational Hepatology **2026** vol. 14(8) | 771–784
DOI: 10.14218/JCTH.2026.00384

Original Article

Plasma Metabolites for Identifying Bacterial Infection in Acute-on-chronic Liver Failure: A Prospective Multicenter Study

Xiaotian Yang[1,2#], Hai Li[3,4,5#], Yan Huang[5,6], Guohong Deng[5,7], Beiling Li[5,8], Xianbo Wang[5,9], Zhongji Meng[5,10], Yubao Zheng[5,11], Yanhang Gao[5,12], Zhiping Qian[5,13], Feng Liu[5,14], Xiaobo Lu[5,15], Yu Shi[5,16], Jia Shang[5,17], Jing Liu[1,2], Hang Jia[1,2], Sumeng Li[1,2], Lining Guo[18*] and Xin Zheng[1,2,5*]

[1]Department of Infectious Diseases, Union Hospital, Tongji Medical College, Huazhong University of Science and Technology, Wuhan, Hubei, China; [2]Joint International Laboratory of Infection and Immunity, Huazhong University of Science and Technology, Wuhan, Hubei, China; [3]Department of Gastroenterology, School of Medicine, Ren Ji Hospital, Shanghai Jiao Tong University, Shanghai, China; [4]Key Laboratory of Gastroenterology and Hepatology, Shanghai Institute of Digestive Disease, Chinese Ministry of Health (Shanghai Jiao Tong University), Shanghai, China; [5]Chinese Chronic Liver Failure Consortium, Shanghai, China; [6]Department of Infectious Diseases, Hunan Key Laboratory of Viral Hepatitis, Xiangya Hospital, Central South University, Changsha, Hunan, China; [7]Department of Infectious Diseases, Southwest Hospital, Third Military Medical University (Army Medical University), Chongqing, China; [8]Hepatology Unit, Department of Infectious Diseases, Nanfang Hospital, Southern Medical University, Guangzhou, Guangdong, China; [9]Center of Integrative Medicine, Beijing Ditan Hospital, Capital Medical University, Beijing, China; [10]Department of Infectious Diseases, Taihe Hospital, Hubei University of Medicine, Shiyan, Hubei, China; [11]Department of Infectious Diseases, The Third Affiliated Hospital, Sun Yat-sen University, Guangzhou, Guangdong, China; [12]Department of Hepatology, The First Hospital of Jilin University, Changchun, Jilin, China; [13]Department of Liver Intensive Care Unit, Shanghai Public Health Clinical Centre, Fudan University, Shanghai, China; [14]Department of Infectious Diseases and Hepatology, The Second Hospital of Shandong University, Jinan, Shandong, China; [15]Infectious Disease Center, The First Affiliated Hospital of Xinjiang Medical University, Urumqi, Xinjiang, China; [16]State Key Laboratory for Diagnosis and Treatment of Infectious Diseases, Collaborative Innovation Center for Diagnosis and Treatment of Infectious Disease, The First Affiliated Hospital, Zhejiang University School of Medicine, Hangzhou, Zhejiang, China; [17]Department of Infectious Diseases, Henan Provincial People's Hospital, Zhengzhou, Henan, China; [18]Shanghai Gan Ning Medical Technology Inc., Pudong New District, Shanghai, China.

Received: May 14, 2026 | **Revised:** June 21, 2026 | **Accepted:** July 06, 2026 | **Published online:** August 03, 2026

Abstract

Background and Aims: Bacterial infection is a key cause of mortality in patients with acute-on-chronic liver failure (ACLF). In this study, we aimed to identify metabolite biomarkers and develop a novel machine learning model for early identification of bacterial infection in ACLF. ***Methods:*** Based on a prospective multicenter cohort from 14 centers, 1,314 patients with acute-on-chronic liver disease were enrolled, including those with ACLF and non-ACLF. Plasma samples at admission were collected for metabolomics profiling. Patients were randomly divided into discovery (n = 921) and validation (n = 393) sets. Machine learning was used to develop diagnostic models. The win ratio method was employed to assess the risk stratification capability of the models. ***Results:*** Bacterial infection occurred in 198 of the 451 ACLF patients and 132 of the 863 non-ACLF patients. Infection altered the plasma metabolome, especially in lipid, amino acid, and xenobiotic metabolic pathways. Models for bacterial infection in ACLF (five metabolites) and non-ACLF (six metabolites) demonstrated superior discrimination in the discovery (AUCs: 0.881 and 0.935, respectively) and validation sets (AUCs: 0.835 and 0.889, respectively) compared with C-reactive protein, white blood cell count, procalcitonin, and the best composite clinical model. Metabolic risk stratification based on the models effectively predicted 90-day outcomes (all-cause death, organ failure, sepsis, new-onset acute decompensation, and systemic inflammatory response syndrome). ***Conclusions:*** Our models based on novel metabolic biomarkers enable identification of patients at high risk of bacterial infection and support risk stratification of 90-day outcomes.

Keywords: Acute-on-chronic liver failure; Liver cirrhosis; Metabolomics; Biomarkers; Machine learning; Infection.

[#]Contributed equally to this work.
[*]**Correspondence to:** Xin Zheng, Department of Infectious Diseases, Union Hospital, Tongji Medical College, Huazhong University of Science and Technology, Wuhan, Hubei 430074, China. ORCID: https://orcid.org/0000-0001-9176-8856. Tel: +86-27-85726026, Fax: +86-27-85726398, E-mail: xinz@hust.edu.cn; Lining Guo, Shanghai Gan Ning Medical Technology Inc., Pudong New District, Shanghai 200433, China. E-mail: liningguo65@gmail.com.

Citation of this article: Yang X, Li H, Huang Y, Deng G, Li B, Wang X, *et al*. Plasma Metabolites for Identifying Bacterial Infection in Acute-on-chronic Liver Failure: A Prospective Multicenter Study. J Clin Transl Hepatol 2026;14(8):771–784. doi: 10.14218/JCTH.2026.00384.

Introduction

Acute-on-chronic liver failure (ACLF) is a clinical syndrome that develops in patients with chronic liver disease who present with acute hepatic dysfunction and is characterized by hepatic and/or extrahepatic organ failure and systemic inflammation.[1] The 90-day mortality for ACLF ranges from 40% to 58%.[2,3] ACLF is associated with concomitant immune dysfunction, which increases susceptibility to bacterial infection.[4,5] Bacterial infection is the most common extrahepatic precipitant and complication of ACLF, affecting nearly 50% of cases.[4] It can trigger a cytokine storm, leading to multiple organ failure and driving a vicious cycle of immunoparalysis and sepsis that substantially elevates mortality.[6,7] Early identification of bacterial infection and antimicrobial intervention are crucial for improving clinical outcomes in this population.

Early and accurate diagnosis of bacterial infection in patients with ACLF remains challenging. Inaccurate diagnosis can lead to overuse of antimicrobials or delays in treatment.[8] Current diagnostic approaches for bacterial infection predominantly rely on conventional biomarkers such as C-reactive protein (CRP), white blood cell count (WBC), and procalcitonin (PCT).[8,9] These indicators can be altered by both infectious and non-infectious causes, and their responses exhibit a temporal lag.[10,11] CRP and PCT are acute-phase reactants. A study showed that bacterial infection does not significantly influence the concentrations of acute-phase proteins in patients with fulminant hepatic failure.[10] Due to the wide range of diagnostic thresholds and the limited time window of acute-phase reactants, their diagnostic accuracy is limited. CRP has low specificity for infection, as it frequently exhibits elevated levels due to systemic inflammation itself.[11,12] PCT has higher specificity but is not suitable for distinguishing infectious from non-infectious inflammation.[11] In the context of liver injury, WBC counts in infected patients are often within the clinically normal range, rendering it inadequate as a standalone diagnostic marker.[12,13] Although pathogen culture remains the diagnostic gold standard for bacterial infection, it has low positivity rates and is unsuitable for routine screening in patients with cirrhosis who have atypical clinical symptoms.[14] None of these methods can capture earlier or more precise signatures of bacterial infection. Previous studies have identified protein signatures associated with infection-related acute decompensation of cirrhosis.[15] However, the metabolomic characteristics of patients with bacterial infection-related ACLF remain unclear. Since our previous work indicated the prognostic value of metabolomics in ACLF,[16] we hypothesized that metabolomics could also identify biomarkers for bacterial infection.

To identify novel biomarkers, we used untargeted metabolomics to analyze a large cohort of plasma samples from patients with acute-on-chronic liver disease (AoCLD). Our objectives were to develop diagnostic models for bacterial infection in ACLF and to assess the models' risk stratification performance for 90-day outcomes. Given the high risk of ACLF progression in non-ACLF (defined in the Materials and methods section) patients with bacterial infection, we analyzed this subgroup separately to complement the primary analysis.

Methods

Patient cohort, data collection, and study design

Patients were recruited from 14 medical centers in the Chinese Acute-on-Chronic Liver Failure study between January 2015 and March 2019. The inclusion criteria for AoCLD were: (1) diagnosis of chronic liver disease; (2) hospitalization for acute liver injury (total bilirubin (TB) > 2 mg/dL, alanine aminotransferase (ALT) or aspartate aminotransferase (AST) > 3× the upper limit of normal); (3) hospitalization for acute decompensation (e.g., gastrointestinal bleeding). The exclusion criteria were: (1) age < 15 or > 80 years; (2) pregnancy; (3) hepatocellular carcinoma or other malignant liver tumors; (4) malignant tumors of other organs; (5) severe extrahepatic diseases; and (6) immunosuppressive therapy.[16] This study was registered at ClinicalTrials.gov (NCT02457637, NCT03641872).

AoCLD patients were classified as ACLF or non-ACLF after enrollment based on clinical follow-up data. ACLF was diagnosed according to the COSSH-ACLF criteria.[14] In patients with cirrhosis, ACLF was defined by the presence of at least one organ failure. In non-cirrhotic patients with advanced fibrosis, ACLF was diagnosed based on the co-occurrence of liver failure (TB > 12 mg/dL) and coagulation failure (international normalized ratio (INR) > 1.5).[8,16] Organ failure was defined as liver, renal, coagulation, circulatory, respiratory, or cerebral failure. The EASL-CLIF ACLF criteria were used to reclassify the samples for further validation of the models.[17] Non-ACLF patients were those with AoCLD who did not meet the corresponding ACLF criteria.

The criteria for infection were based on evidence of bacterial infection within 48 h of admission.[8] The inclusion criteria were: (1) pulmonary infection: an infectious focus shown on X-ray or CT, or a positive bacterial culture obtained from sputum, tracheal aspirate, or bronchoalveolar lavage fluid; (2) urinary tract infection: urine leukocyte count > 10/high-power field, positive bacterial Gram stain, or positive midstream urine culture; (3) spontaneous bacterial peritonitis (SBP): absolute neutrophil count in ascites ≥ 250/mm^3; (4) spontaneous bacteremia: positive blood culture; (5) skin and soft tissue infection: clinical manifestations of infection with swelling, erythema, fever, and skin tenderness; (6) other bacterial infections (e.g., cholangitis). Patients with fungal or non-hepatotropic viral infections were excluded from this study.[18,19]

Demographic information, etiological data, clinical symptoms, complications, laboratory tests, and treatments after admission were recorded. EDTA plasma samples collected within 48 h of admission and before empirical antibiotic therapy were obtained and stored at −80 °C. The study design is summarized in Figure 1. After excluding 28 patients who underwent liver transplantation and 44 patients with fungal or non-hepatotropic viral infections and missing infection data, the final analysis included 1,314 of the initial 1,386 patients. We applied machine learning (ML) and statistical analyses to identify candidate biomarkers in the discovery set. Model validation and prognostic risk stratification assessment were conducted in the validation set.

Metabolomics profiling

Untargeted metabolomics analysis was based on the Discovery HD4 metabolomics platform from Metabolon (Durham, North Carolina, USA). The detailed methods were previously reported and are provided in the Supplementary File 1.[16] In brief, samples were extracted with methanol to precipitate proteins. The supernatant was divided into four aliquots following centrifugation, and each aliquot was analyzed using a distinct ultra-high-performance liquid chromatography/tandem mass spectrometry (UHPLC-MS/MS) method. Two aliquots were analyzed using separate reverse-phase (RP) UPLC-MS/MS methods with positive-ion mode electrospray ionization (ESI), one aliquot using RP/UPLC-MS/MS with negative-ion mode ESI, and one aliquot using hydrophilic interaction liquid chromatography/UPLC-MS/MS with negative-ion

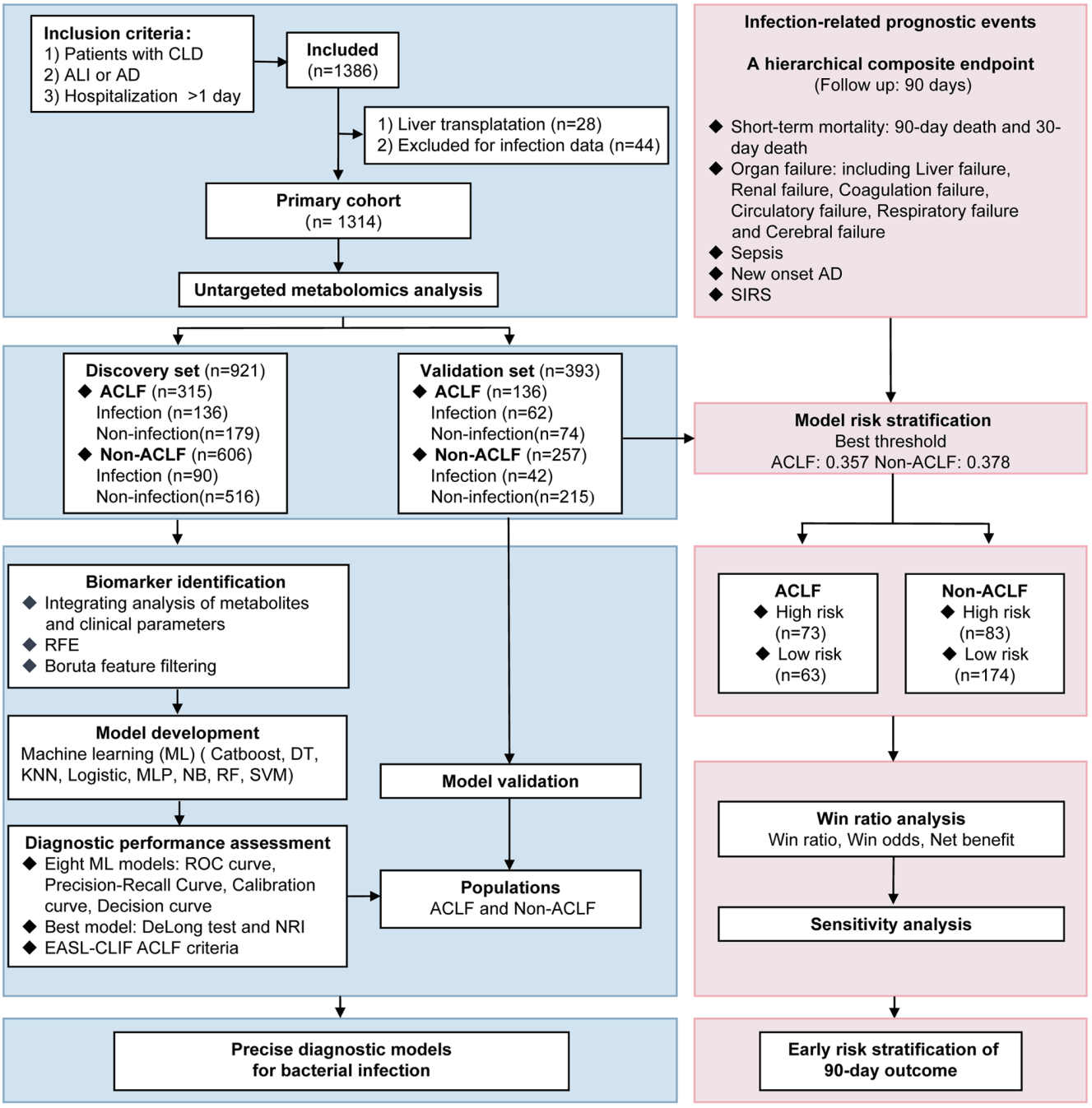

Fig. 1. Research flowchart. ACLF, acute-on-chronic liver failure; AD, acute decompensation; ALI, acute liver injury; AUC, area under the curve; CatBoost, Categorical boosting; CLD, chronic liver disease; DT, decision tree; EASL-CLIF, European Association for the Study of the Liver - Chronic Liver Failure; KNN, K-nearest neighbor; Logistic, logistic regression; ML, machine learning; MLP, multilayer perceptron; NB, naive bayes; NRI, net reclassification improvement; RF, random forest; RFE, recursive feature elimination; ROC, receiver operating characteristic; SIRS, systemic inflammatory response syndrome; SVM, support vector machine.

mode ESI. Metabolite identification, quantification, curation, normalization, and quality control were performed using the platform's software.

Statistical analysis

Statistical analyses were performed using R (version 4.4.3, http://www.r-project.org) and DecisionLinnc software. Normally distributed continuous variables were compared using Student's t-test, while the Mann-Whitney U test was used for non-normally distributed variables. Categorical variables were compared using the chi-square test or Fisher's exact test. *P*-values were adjusted using the Benjamini-Hochberg method to control the false discovery rate (FDR). For untargeted metabolomics data, metabolites with >80% missing values were excluded. Remaining missing values were imputed using half of the minimum detected value for the

corresponding metabolite. The metabolomics data were $\log_2$-transformed, and differential metabolite expression was evaluated by calculating fold change, *P*-values, and estimated FDR. Spearman correlation analysis was used to evaluate relationships between variables. The composite endpoint of infection-related prognostic events was assessed as having hierarchical clinical importance using the win ratio method described in the Supplementary File 1.[20] All statistical tests were two-tailed, and statistical significance was defined as $P < 0.05$.

Model development, evaluation, and interpretation

The cohort was randomly split into discovery and validation sets in a 7:3 ratio using stratified random sampling according to infection status. Feature selection was performed using the Boruta algorithm. Within the confirmed variable set identified by Boruta, recursive feature elimination (RFE) was applied to determine the optimal number of variables in the selected feature subset. To ensure translational applicability, features were further filtered based on the availability of corresponding chemical standards, yielding the final feature subset.

Eight ML algorithms were used to predict the risk of bacterial infection: categorical boosting (CatBoost), multilayer perceptron (MLP), support vector machine (SVM), decision tree (DT), random forest (RF), naive Bayes (NB), logistic regression (LR), and k-nearest neighbors (KNN). The prevalence of bacterial infection was relatively balanced in the ACLF group (0.439) but imbalanced in the non-ACLF group (0.153). Therefore, the synthetic minority over-sampling technique (SMOTE) was applied to the discovery set of the non-ACLF group to balance the minority class, while the original distribution was retained in the ACLF dataset. The optimal hyperparameters for each model were determined through grid search using accuracy as the metric, supplemented by manual tuning (Supplementary Table 1). Each model was developed using the final feature subset and optimal hyperparameters. The final algorithm was selected based on evaluation metrics including discrimination, calibration, and overfitting assessment.

Model performance was evaluated using the area under the receiver operating characteristic curve (AUROC), precision-recall curves, accuracy, specificity, recall, precision, and F1 score. Calibration was assessed using calibration curves. Clinical utility was estimated using decision curve analysis (DCA). AUROC differences were compared using DeLong's test, while net reclassification improvement (NRI) quantified the improvement in discrimination over previous benchmarks. The Youden index was used to determine optimal model thresholds. The SHapley Additive exPlanations (SHAP) method was used to interpret model predictions and quantify the contribution of key features.

Results

Patient characteristics

Among the 1,314 enrolled patients with AoCLD, 451 met the COSSH-ACLF criteria. Bacterial infection occurred in 198 (43.90%) ACLF patients and 132 (15.30%) non-ACLF patients. Baseline characteristics were compared between the infected and non-infected groups (Table 1). In ACLF patients, no significant differences in sex, age (median age: 49.20 vs. 48.19 years, $P = 0.735$), or cirrhosis (84.34% vs. 80.63%, $P = 0.306$) were observed between the infected and uninfected groups. Among non-ACLF patients, those with infection were older (median age: 53.0 vs. 49.0 years, $P < 0.001$) and had a higher prevalence of cirrhosis (84.85% vs. 65.12%, $P < 0.001$). HBV was the primary etiology of ACLF, accounting for 355 (78.71%) cases. The proportion of alcohol-related cases was higher in ACLF patients with bacterial infection than in those without (54 (27.27%) vs. 46 (18.18%), $P = 0.021$). In the non-ACLF population, the proportion of HBV infection was lower in patients with bacterial infection than in those without (79 (59.85%) vs. 552 (75.51%), $P < 0.001$), whereas the proportion of alcohol-related etiology was higher in the infected group compared with the non-infected group (42 (31.8%) vs. 149 (20.38%), $P = 0.004$). In both the ACLF and non-ACLF cohorts, infected patients exhibited higher rates of jaundice and ascites as acute decompensation events than uninfected patients (all $P < 0.001$). Laboratory parameters also differed significantly: infected patients exhibited elevated levels of CRP, WBC, PCT, neutrophils, neutrophil-to-lymphocyte ratio (NLR), prothrombin time, INR, TB, AST/ALT ratio, blood urea nitrogen, and creatinine, whereas albumin and sodium were significantly decreased (all $P < 0.05$).

The distribution of bacterial infection types was similar between ACLF and non-ACLF patients. Pulmonary infection was the predominant type (ACLF: 70.71%, non-ACLF: 71.21%), followed by SBP (15.66%, 12.88%), other infections, urinary tract infection, skin and soft tissue infection, and spontaneous bacteremia. Among pathogens isolated via bacterial culture, Gram-negative bacteria (ACLF: 53.66%, non-ACLF: 57.58%) were the most prevalent, followed by Gram-positive bacteria (ACLF: 34.15%, non-ACLF: 24.24%) and mixed infections (Supplementary Table 2).

Plasma metabolic profiles altered by bacterial infection in ACLF and non-ACLF

Untargeted metabolomics identified 1,072 known metabolites, of which 176 detected in fewer than 20% of samples were excluded. Orthogonal partial least squares discriminant analysis (OPLS-DA) of the remaining 896 metabolites distinguished infected from uninfected patients in both the ACLF and non-ACLF groups (Supplementary Fig. 1). Consistent with prior findings, the plasma metabolome differed significantly between ACLF and non-ACLF patients.[16] Hence, we analyzed the two subgroups separately in subsequent analyses. A total of 400 metabolites (44.6%) in the ACLF group and 481 (53.7%) in the non-ACLF group showed significant differences between infected and uninfected patients, respectively (Fig. 2A and B).

The metabolites formed four clusters (C1–C4) during disease progression (Fig. 2C). Metabolites in C1 (e.g., thyroxine) showed a sustained decrease with both bacterial infection and ACLF progression, whereas metabolites in C3 (e.g., pipecolate and 2-isopropylmalate) exhibited a sustained increase. Metabolites in C2 and C4 were associated with bacterial infection independent of ACLF status, characterized by elevated levels of C2 (e.g., orotate and ribitol) and reduced levels of C4 (e.g., sphingosine-1-phosphate (S1P)) in infected patients. These clusters were enriched in superpathways including lipids, amino acids, and xenobiotics (Supplementary Fig. 2).

Bacterial infection remodeled the ACLF plasma metabolome, particularly affecting pathways related to lipid biosynthesis, amino acid catabolism, and pyrimidine metabolism (Fig. 2D). Among the top 40 metabolites, 13 were lipids, including lysophospholipids, phospholipids, sphingomyelins, and sphingosines. These lipids were generally downregulated in patients with infection. Given their roles in maintaining membrane integrity and lipid-mediated immune signal transduction, these changes may reflect membrane remodeling or degradation during infection in ACLF. For example, re-

Table 1. Comparison of baseline clinical parameters between infected and uninfected in the ACLF and non-ACLF groups

Characteristics	ACLF (n = 451)	ACLF		*P*-value
		Infection (n = 198)	Non-infection (n = 253)	
Age, Median (Q1, Q3)	48.67 (41.00–57.00)	49.20 (42.00–57.22)	48.19 (40.91–56.00)	0.735
Male, n (%)	365 (80.93)	161 (81.31)	204 (80.63)	0.855
Cirrhosis, n (%)	371 (82.26)	167 (84.34)	204 (80.63)	0.306
Etiology, n (%)				
HBV	355 (78.71)	156 (78.79)	199 (78.66)	0.973
HCV	3 (0.67)	1 (0.51)	2 (0.79)	0.711
HEV	16 (3.55)	3 (1.52)	13 (5.14)	0.039
Alcohol	100 (22.17)	54 (27.27)	46 (18.18)	0.021
Autoimmune	33 (7.32)	13 (6.57)	20 (7.91)	0.588
NAFLD	16 (3.55)	3 (1.52)	13 (5.14)	0.039
Schistosomiasis	4 (0.89)	2 (1.01)	2 (0.79)	0.805
Cryptogenic	18 (3.99)	11 (5.56)	7 (2.77)	0.133
Type of AD, n (%)				
HE				0.775
0	371 (82.26)	162 (81.82)	209 (82.61)	
1	22 (4.88)	8 (4.04)	14 (5.53)	
2	30 (6.65)	15 (7.58)	15 (5.93)	
3	17 (3.77)	9 (4.55)	8 (3.16)	
4	11 (2.44)	4 (2.02)	7 (2.77)	
Jaundice	404 (89.58)	188 (94.95)	216 (85.38)	<0.001
Ascites	284 (62.97)	158 (79.80)	126 (49.80)	<0.001
GI bleeding	31 (6.87)	13 (6.57)	18 (7.11)	0.819
Laboratory data, M (Q_1, Q_3)				
TB (mg/dL)	19.57 (13.11–27.37)	22.18 (14.96–30.06)	17.77 (12.39–23.78)	<0.001
INR	2.01 (1.55–2.61)	2.09 (1.66–2.69)	1.86 (1.44–2.50)	0.002
Cr (mg/dL)	0.85 (0.68–1.13)	0.88 (0.72–1.27)	0.82 (0.67–1.04)	0.002
BUN (mmol/L)	4.59 (3.27–7.27)	5.23 (3.44–9.23)	4.20 (3.11–6.15)	<0.001
ALT (U/L)	154.60 (54.10–481.00)	123.00 (53.00–388.00)	180.60 (55.20–562.00)	0.151
AST (U/L)	169.60 (82.40–363.00)	153.35 (87.00–342.00)	182.00 (79.00–400.00)	0.904
AST/ALT	1.11 (0.71–1.74)	1.21 (0.79–2.00)	1.00 (0.69–1.62)	0.002
ALB (g/L)	30.80 (27.20–33.80)	29.70 (25.80–33.10)	31.11 (28.30–34.50)	0.001
ALP (U/L)	142.00 (109.00–189.00)	143.50 (103.53–194.05)	141.50 (112.00–186.00)	0.797
γ-GT (U/L)	79.15 (47.00–123.00)	80.10 (52.00–138.95)	78.45 (44.90–119.00)	0.387
WBC (×109/L)	6.66 (4.70–9.46)	7.88 (5.70–11.37)	5.80 (4.21–8.15)	<0.001
PLT (×109/L)	100.00 (65.00–143.00)	86.00 (60.00–131.00)	105.00 (68.00–151.00)	0.010
MAP (mmHg)	89.00 (82.33–96.00)	87.67 (81.00–94.33)	90.33 (83.33–97.00)	0.002
NLR ratio	3.84 (2.41–6.39)	4.92 (2.81–8.18)	3.27 (2.26–5.16)	<0.001
HGB (g/L)	119.00 (101.00–134.00)	116.50 (98.00–129.00)	123.00 (105.00–137.00)	0.005
N (×109/L)	4.45 (3.03–6.69)	5.59 (3.86–8.93)	3.85 (2.61–5.33)	<0.001
L (×109/L)	1.18 (0.78–1.63)	1.19 (0.74–1.65)	1.17 (0.78–1.62)	0.832
K + (mmol/L)	3.83 (3.50–4.20)	3.80 (3.39–4.16)	3.90 (3.58–4.22)	0.030
Na+ (mmol/L)	136.55 (133.50–139.00)	135.00 (131.30–137.90)	137.50 (135.10–139.70)	<0.001
CRP (mg/L)	12.60 (6.85–19.90)	17.55 (11.40–30.40)	9.64 (5.90–14.99)	<0.001
PCT (ng/mL)	0.56 (0.28–1.03)	0.71 (0.45–1.26)	0.47 (0.23–0.77)	<0.001
PT (s)	23.30 (17.80–29.80)	24.75 (20.00–30.60)	21.40 (16.80–28.00)	<0.001

(continued)

Table 1. *(continued)*

Characteristics	Non-ACLF (n = 863)	Non-ACLF		*P*-value
		Infection (n = 132)	Non-infection (n = 731)	
Age, Median (Q1, Q3)	49.00 (40.00–58.22)	53.00 (43.46–62.69)	49.00 (39.00–57.42)	<0.001
Male, n (%)	615 (71.26)	93 (70.45)	522 (71.41)	0.824
Cirrhosis, n (%)	588 (68.13)	112 (84.85)	476 (65.12)	<0.001
Etiology, n (%)				
HBV	631 (73.12)	79 (59.85)	552 (75.51)	<0.001
HCV	9 (1.04)	3 (2.27)	6 (0.82)	0.131
HEV	8 (0.93)	1 (0.76)	7 (0.96)	0.825
Alcohol	191 (22.13)	42 (31.82)	149 (20.38)	0.004
Autoimmune	96 (11.12)	10 (7.58)	86 (11.76)	0.159
NAFLD	38 (4.40)	5 (3.79)	33 (4.51)	0.708
Schistosomiasis	8 (0.93)	3 (2.27)	5 (0.68)	0.080
Cryptogenic	14 (1.62)	4 (3.03)	10 (1.37)	0.164
Type of AD, n (%)				
HE				0.759
0	810 (93.86)	126 (95.45)	684 (93.57)	
1	29 (3.36)	4 (3.03)	25 (3.42)	
2	21 (2.43)	2 (1.52)	19 (2.60)	
3	3 (0.35)	0 (0.00)	3 (0.41)	
4	0 (0.00)	0 (0.00)	0 (0.00)	
Jaundice	247 (28.62)	60 (45.45)	187 (25.58)	<0.001
Ascites	385 (44.61)	97 (73.48)	288 (39.40)	<0.001
GI bleeding	133 (15.41)	19 (14.39)	114 (15.60)	0.725
Laboratory data, M (Q_1, Q_3)				
TB (mg/dL)	2.53 (1.29–5.72)	4.48 (2.14–8.91)	2.27 (1.25–5.15)	<0.001
INR	1.34 (1.17–1.59)	1.53 (1.32–1.80)	1.31 (1.15–1.55)	<0.001
Cr (mg/dL)	0.77 (0.63–0.89)	0.81 (0.64–1.04)	0.76 (0.63–0.88)	0.028
BUN (mmol/L)	4.50 (3.50–6.00)	5.01 (3.73–7.33)	4.40 (3.41–5.89)	0.002
ALT (U/L)	68.00 (30.00–308.00)	42.20 (26.00–119.55)	79.10 (30.40–347.00)	<0.001
AST (U/L)	84.90 (44.00–231.00)	73.00 (45.60–146.10)	88.00 (43.80–246.00)	0.170
AST/ALT	1.16 (0.72–1.65)	1.47 (1.05–2.06)	1.10 (0.67–1.57)	<0.001
ALB (g/L)	32.30 (28.19–36.80)	28.20 (24.45–32.10)	33.10 (29.10–37.70)	<0.001
ALP (U/L)	120.00 (88.90–163.00)	132.88 (92.00–166.00)	119.00 (88.00–163.00)	0.165
γ-GT (U/L)	87.00 (35.00–166.00)	82.00 (34.00–161.00)	87.00 (36.00–167.00)	0.457
WBC (×109/L)	4.60 (3.31–6.07)	5.95 (3.96–8.49)	4.49 (3.17–5.89)	<0.001
PLT (×109/L)	93.00 (58.00–151.00)	77.00 (51.00–122.50)	97.00 (60.00–154.00)	0.003
MAP (mmHg)	88.33 (83.33–95.33)	87.00 (80.83–93.67)	88.67 (83.33–95.67)	0.040
NLR ratio	2.11 (1.36–3.32)	3.46 (2.07–6.20)	1.98 (1.31–2.94)	<0.001
HGB (g/L)	117.00 (98.00–135.00)	109.50 (85.50–123.00)	119.00 (99.00–136.00)	<0.001
N (×109/L)	2.60 (1.79–3.81)	3.77 (2.38–6.46)	2.45 (1.70–3.55)	<0.001
L (×109/L)	1.22 (0.81–1.77)	1.11 (0.76–1.78)	1.24 (0.83–1.77)	0.240
K + (mmol/L)	3.89 (3.57–4.15)	3.80 (3.40–4.12)	3.90 (3.60–4.15)	0.135

(continued)

Table 1. *(continued)*

Characteristics	Non-ACLF (n = 863)	Non-ACLF		*P*-value
		Infection (n = 132)	Non-infection (n = 731)	
Na+ (mmol/L)	139.00 (136.90–141.05)	137.10 (133.90–140.00)	139.10 (137.00–141.40)	<0.001
CRP (mg/L)	5.90 (2.80–11.61)	13.35 (7.49–33.25)	4.80 (2.50–10.30)	<0.001
PCT (ng/mL)	0.17 (0.08–0.36)	0.28 (0.15–0.56)	0.14 (0.07–0.32)	<0.001
PT (s)	15.60 (13.60–18.20)	18.05 (15.55–20.70)	15.20 (13.30–17.80)	<0.001

ACLF, acute-on-chronic liver failure; AD, acute decompensation; ALT, alanine aminotransferase; AST, aspartate aminotransferase; AST/ALT, aspartate aminotransferase to alanine aminotransferase ratio; ALB, albumin; ALP, alkaline phosphatase; BUN, blood urea nitrogen; CRP, C-reactive protein; Cr, creatinine; GI bleeding, gastrointestinal bleeding; γ-GT, γ-glutamyl transferase; HE, hepatic encephalopathy; HGB, hemoglobin; HBV, hepatitis B virus; HCV, hepatitis C virus; HEV, hepatitis E virus; INR, international normalized ratio; L, lymphocyte count; MAP, mean arterial pressure; N, neutrophil count; NLR, neutrophil-to-lymphocyte ratio; NAFLD, nonalcoholic fatty liver disease; PLT, platelet count; PCT, procalcitonin; PT, prothrombin time; TB, total bilirubin; WBC, white blood cell count.

duced S1P levels have been associated with sepsis-induced liver injury.[21] Another 13 metabolites belonged to amino acid metabolism. Among these, thyroxine was significantly downregulated, whereas others (e.g., pipecolate) were upregulated. Thyroxine can enhance leukocyte function during bacterial pneumonia, and hypothyroidism is a known risk factor for infection.[22] Elevated levels of pipecolate reflected both infection and ACLF progression and indicated perturbed lysine metabolism.[23] Of the remaining 14 metabolites, 6 nucleotides (e.g., orotate) and 2 carbohydrates (e.g., ribitol) were all upregulated.[24] The other 6 metabolites consisted of 3 xenobiotics (e.g., 2-isopropylmalate, upregulated) and 3 cofactors and vitamins (e.g., gamma-CEHC, downregulated). KEGG enrichment analysis highlighted disturbed metabolic pathways in ACLF patients with bacterial infection (Supplementary Fig. 3), including pyrimidine metabolism, characterized by increased levels of 3-ureidopropionate, orotate, and thymine (Fig. 2D). Pyrimidine derivatives possess antimicrobial and antiviral properties and are modulated during host–pathogen interactions.[24] Other core metabolic pathways were also perturbed, including pantothenate and CoA biosynthesis and beta-alanine metabolism. Pantothenate and its derivative CoA are central coenzymes in cellular metabolism. Bacteria can regulate virulence gene expression by modulating pantothenate synthesis via the beta-alanine pathway.[25]

We investigated the associations between the top 10 infection-related metabolites and key clinical indicators. In ACLF, metabolites (1-linoleoyl-GPE (18:2), thyroxine, pipecolate, S1P, and 2-isopropylmalate) were significantly correlated with inflammatory markers, including CRP, PCT, WBC, neutrophils, and NLR. In non-ACLF, a distinct set (3-ureidopropionate, orotate, ribitol, and 3-phenylpropionate) showed similar associations (Fig. 2E and F).

In summary, the disturbed plasma metabolome elucidates the link between infection-induced metabolic stress and immune homeostasis imbalance, emphasizing the potential of metabolite biomarkers for monitoring organ function and the interplay between host immunity and pathogen infection.

Model development and validation for bacterial infection in ACLF

Among patients who met the COSSH-ACLF criteria, concurrent bacterial infection was present in 136 of 315 in the discovery set and 62 of 136 in the validation set. Baseline clinical parameters are summarized in Supplementary Table 3.

In the initial exploration (Fig. 3A), the top 40 metabolites exhibited independent diagnostic value (AUCs: 0.650–0.773). Candidate metabolite biomarkers were screened for importance using the Boruta algorithm to identify a confirmed variable set (Fig. 3B). Subsequently, feature reduction was performed using RFE to determine the minimum number of variables required for stable performance (Supplementary Table 4). The final feature subset was further refined based on both the availability of chemical standards and statistical significance (Supplementary Fig. 4). Five metabolites (thyroxine, 2-isopropylmalate, pipecolate, 1-linoleoyl-GPE (18:2), and S1P) were identified as the optimal biomarkers.

Eight ML algorithms were trained using a five-metabolite panel. The CatBoost model demonstrated superior performance in the discovery set (AUC: 0.881 (95% CI: 0.844–0.918)) and validation set (AUC: 0.835 (95% CI: 0.769–0.902)) (Fig. 3C and Supplementary Table 5). The CatBoost model was well calibrated (Brier score: 0.145), confirming the reliability of its probability estimates (Supplementary Figs. 5 and 6). DCA showed that the CatBoost model provided a higher net benefit across a wide range of threshold probabilities than the other models (Fig. 3D).

Model development and validation for the diagnosis of bacterial infection in non-ACLF

Among the 863 non-ACLF patients, concurrent bacterial infection was found in 89 of 606 in the discovery set and 43 of 257 in the validation set. Baseline clinical parameters are summarized in Supplementary Table 6.

Individual metabolites showed moderate diagnostic value (AUCs: 0.689–0.784, Fig. 4A). The above steps were repeated to identify a six-metabolite panel (3-phenylpropionate, ribitol, 1-linoleoyl-GPC (18:2), orotate, S1P, and 1-carboxyethylphenylalanine) for model training (Fig. 4B, Supplementary Fig. 7, and Supplementary Table 7). Given the class imbalance of positive events, we applied the SMOTE method to the discovery set. Model validation was conducted on the unsampled validation set.

Among eight ML algorithms, the six-metabolite CatBoost model demonstrated superior overall performance in the discovery set (AUC: 0.935 (95% CI: 0.920–0.949)) and validation set (AUC: 0.889 (95% CI: 0.859–0.920)) (Fig. 4C and Supplementary Table 8). Calibration curves showed that the model was acceptable at reasonable thresholds, with a Brier score of 0.136 (Supplementary Fig. 8). DCA indicated that the model had good clinical utility (Fig. 4D).

Model comparison and sensitivity analysis

We reclassified patients according to the EASL-CLIF ACLF criteria and compared baseline parameters between infected and uninfected patients with ACLF (Supplementary Table 9). The performance of the ACLF bacterial infection model remained robust under this reclassification, with AUCs of 0.872 (95% CI: 0.828–0.916) in the discovery set (Fig. 5A) and 0.824 (95% CI: 0.743–0.906) in the validation set (Fig. 5B).

We used DeLong's test and NRI to compare the five-me-

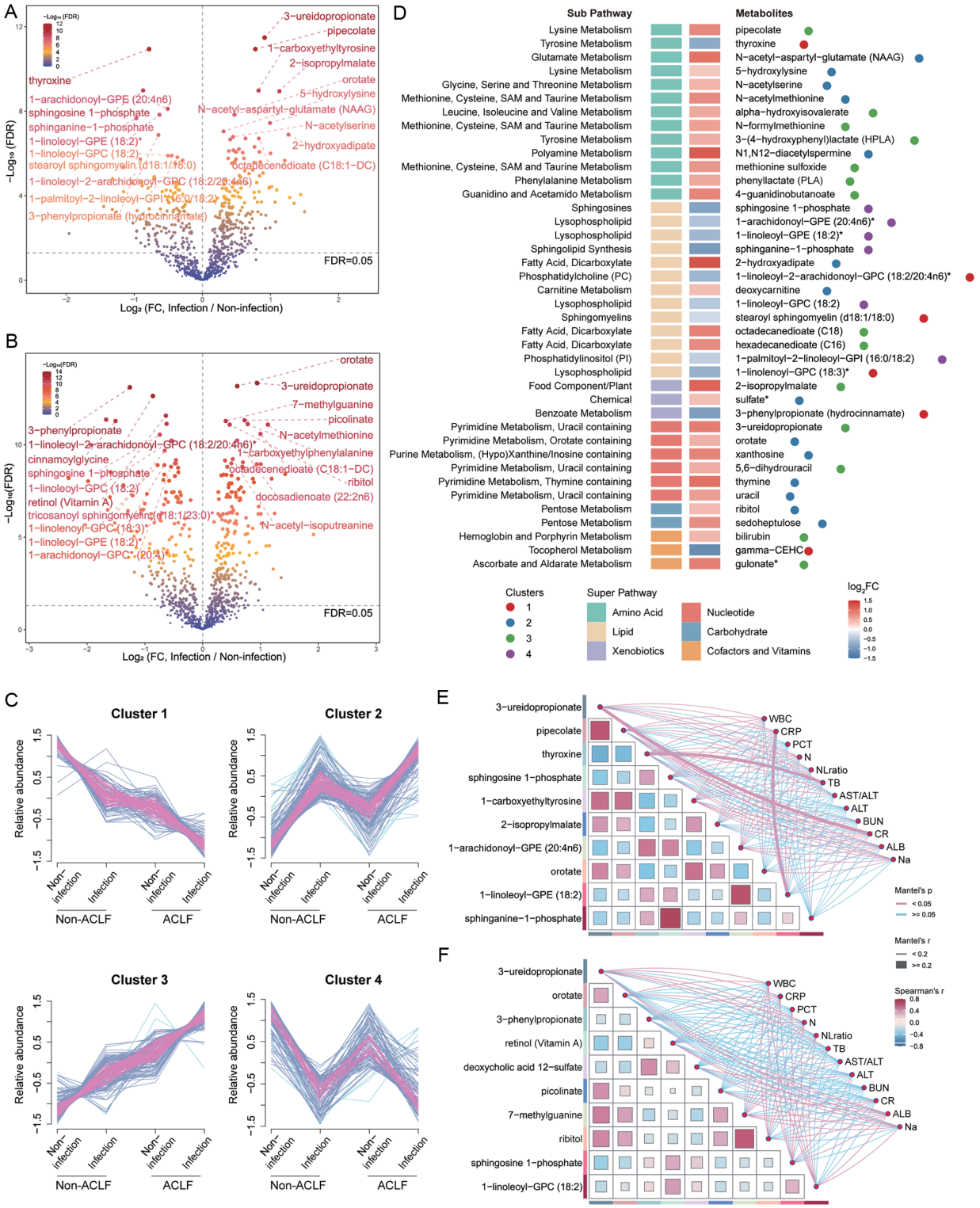

Fig. 2. Plasma metabolomic profiles altered by bacterial infection in ACLF and non-ACLF. (A, B) Volcano plot of differential metabolites between infected and uninfected patients in (A) ACLF or (B) non-ACLF. (C) Mfuzz clustering revealing trajectories of differential plasma metabolites during infection or ACLF progression. (D) Metabolic pathways associated with infection in ACLF. The right color bar indicates the log_2(FC) of each metabolite in the infection group versus the non-infection controls. The left color bar and columns denote the superpathway and subpathway classifications. (E, F) Spearman's correlation analysis between the top 10 infection-related metabolites and clinical indicators. (E) Correlations in ACLF. (F) Correlations in non-ACLF. ACLF, acute-on-chronic liver failure; ALT, alanine aminotransferase; AST/ALT, aspartate to alanine aminotransferase ratio; ALB, albumin; BUN, blood urea nitrogen; CRP, C-reactive protein; CR, creatinine; FC, fold change; N, neutrophil count; NL ratio, neutrophil-lymphocyte ratio; PCT, procalcitonin; TB, total bilirubin; WBC, white blood cell count.

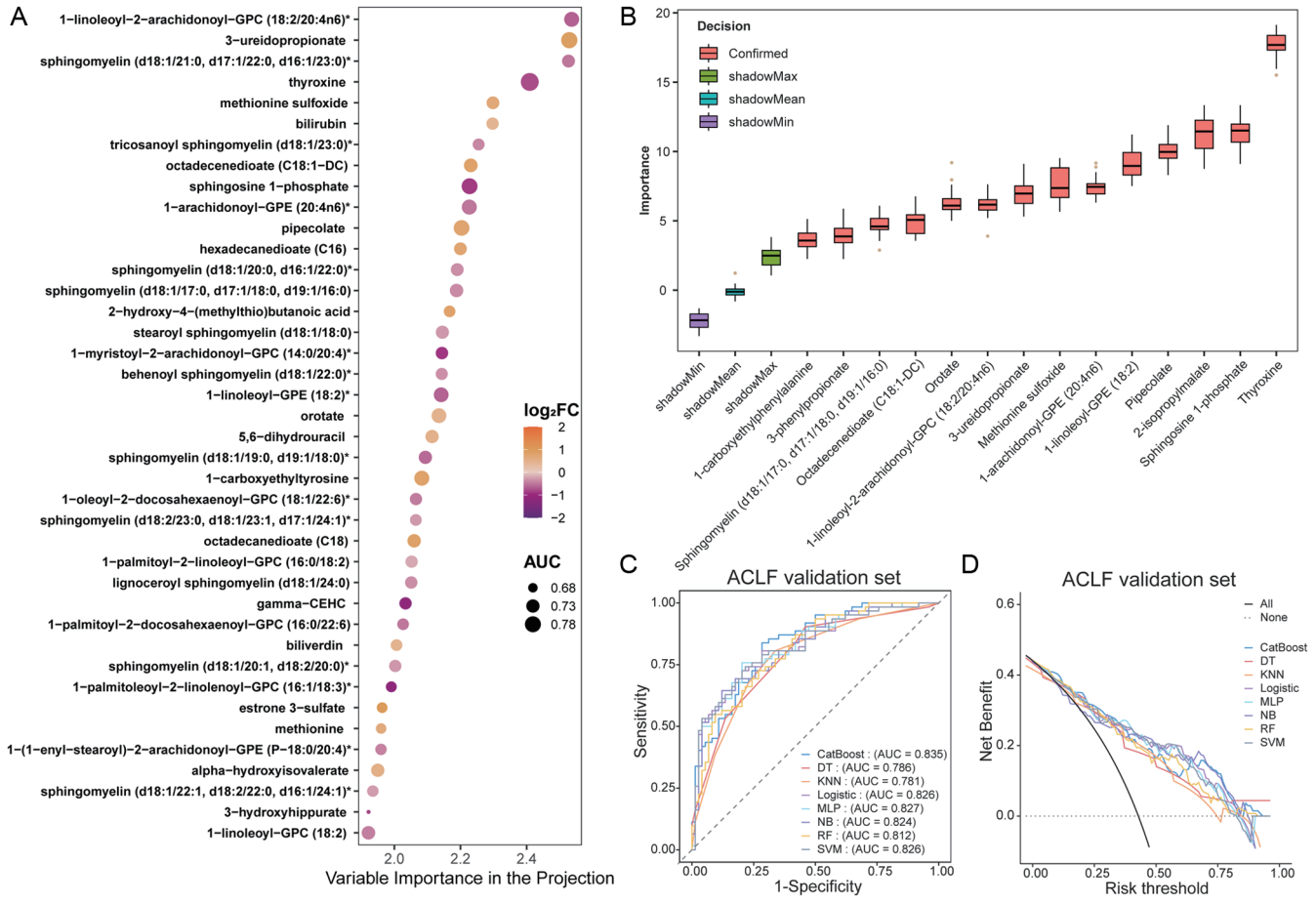

Fig. 3. Identification of metabolic biomarkers for the diagnosis of bacterial infection in ACLF. (A) Top 40 metabolites in ACLF patients with infection versus those without. (B) Boruta box plot for variable importance. (C) ROC curves of the five-metabolite model (thyroxine, 2-isopropylmalate, pipecolate, 1-linoleoyl-GPE (18:2), and sphingosine-1-phosphate). (D) DCA curves. ACLF, acute-on-chronic liver failure; AUC, area under the curve; CatBoost, Categorical boosting; DT, decision tree; FC, fold change; KNN, K-nearest neighbor; Logistic, logistic regression; ML, machine learning; MLP, multilayer perceptron; NB, naive bayes; RF, random forest; SVM, support vector machine.

tabolite model with conventional indicators (CRP and WBC) and with the combined model (five metabolites + CRP) (Fig. 5C). The discrimination of the five-metabolite model was better than that of conventional clinical indicators (AUCs: 0.665–0.691, all $P < 0.05$) and showed no significant difference compared with the combined model (AUC: 0.840 (95% CI: 0.774–0.905), $P = 0.855$; NRI: 0.008, $P = 0.910$) in the validation set (Supplementary Tables 10 and 11).

We compared the performance of the six-metabolite model with that of conventional indicators (CRP, neutrophils, or PCT) and the combined model (six metabolites + CRP) (Fig. 5D). The six-metabolite model outperformed conventional indicators (AUCs: 0.624–0.782, all $P < 0.001$) and showed a significant improvement in AUC but a non-significant NRI compared with the combined model (AUC: 0.929 (95% CI: 0.905–0.953), $P < 0.001$; NRI: 0.056, $P = 0.082$) in the validation set (Supplementary Tables 12 and 13). This discrepancy arose because DeLong's test evaluates overall discrimination across all thresholds, whereas NRI assesses reclassification improvement at specific cutoffs.

To further explore the diagnostic information that metabolites add beyond the clinical model, we used RFE to evaluate all clinical indicators and selected the optimal combination (Supplementary Tables 14 and 15). Metabolomics models outperformed the best composite clinical model in both ACLF (AUC: 0.752 (0.670–0.834), $P < 0.05$) and non-ACLF (AUC: 0.823 (0.784–0.863), $P < 0.05$) patients in the validation set (Supplementary Table 16).

We conducted a sensitivity analysis using microbiologically confirmed cases. Pathogens were isolated from 82 of 198 ACLF cases and 66 of 132 non-ACLF cases. Models for bacterial infection in ACLF and non-ACLF remained robust in the discovery (AUCs: 0.948 and 0.962, respectively) and validation sets (AUCs: 0.869 and 0.881, respectively) (Supplementary Table 17).

We analyzed model performance across ACLF grades. Of the 451 patients with ACLF, 311 had ACLF-1, 110 had ACLF-2, and 30 had ACLF-3. Model performance varied slightly across grades and remained generally robust. The AUCs for the discovery and validation sets were 0.880 and 0.824 for ACLF-1, 0.947 and 0.830 for ACLF-2, and 0.961 and 0.859 for ACLF-3, respectively (Supplementary Table 18).

Baseline metabolic risk stratification for 90-day outcomes

During the 90-day follow-up, the bacterial infection group had significantly higher 90-day mortality than the non-infection group in both ACLF (infection: 45.45%, non-infection:

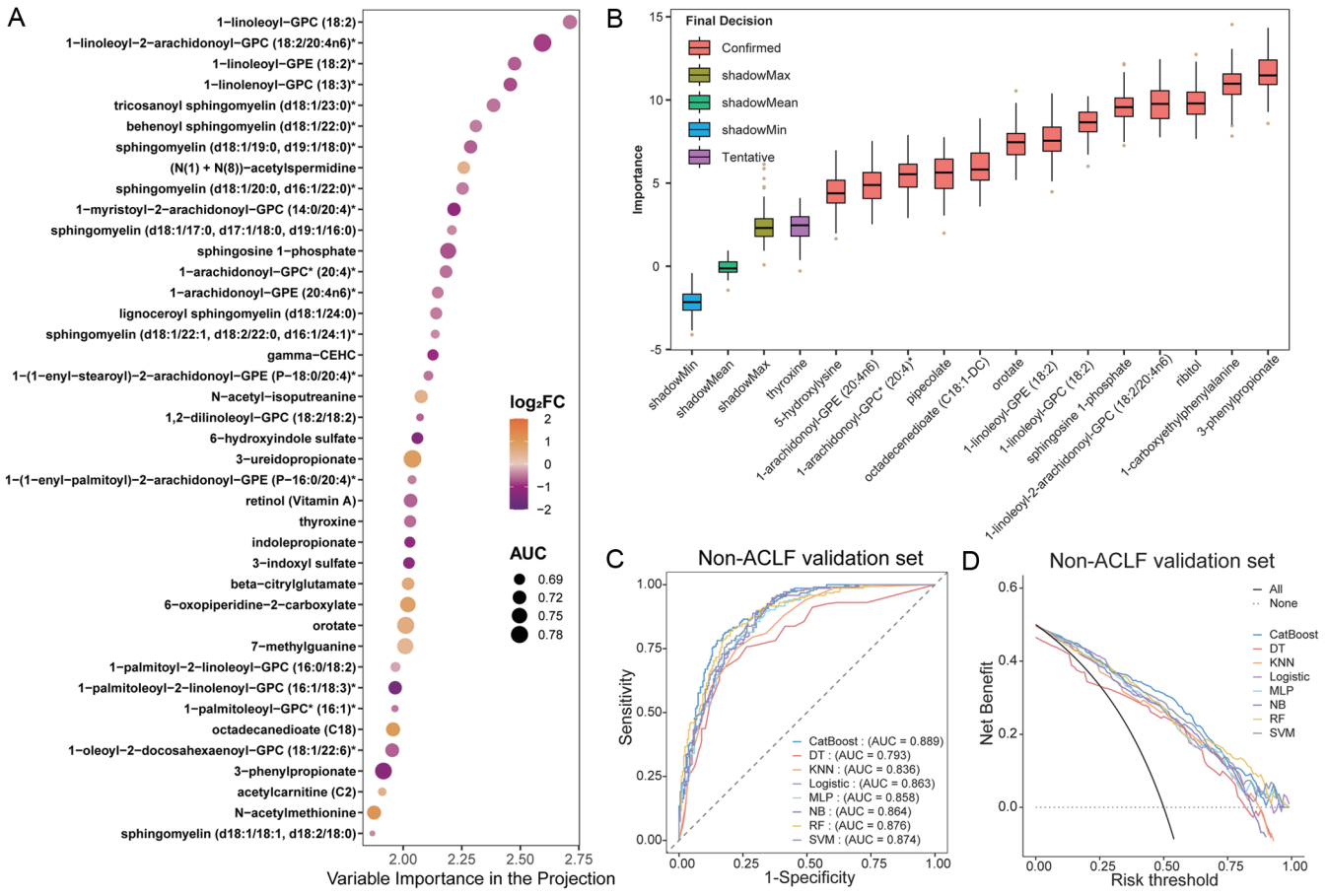

Fig. 4. Identification of metabolic biomarkers for the diagnosis of bacterial infection in non-ACLF. (A) Top 40 metabolites in non-ACLF patients with infection versus those without. (B) Boruta box plot for variable importance. (C) ROC curves of the six-metabolite model (3-phenylpropionate, ribitol, 1-linoleoyl-GPC (18:2), orotate, sphingosine-1-phosphate, and 1-carboxyethylphenylalanine). (D) DCA curves. ACLF, acute-on-chronic liver failure; AUC, area under the curve; CatBoost, Categorical boosting; DT, decision tree; FC, fold change; KNN, K-nearest neighbor; Logistic, logistic regression; ML, machine learning; MLP, multilayer perceptron; NB, naive bayes; RF, random forest; SVM, support vector machine.

22.53%) and non-ACLF (infection: 12.12%, non-infection: 3.69%) populations (all $P < 0.0001$, Supplementary Fig. 9). We employed the win ratio method to assess the risk stratification capacity of the diagnostic model for 90-day outcomes. In this approach, for each patient pair, the first step was to determine whether the high-risk patient died before the low-risk patient. Pairs that remained tied were then compared for non-fatal events in a prespecified order of clinical importance.[20]

Patients with ACLF in the validation set were stratified into high infection-related risk (n = 73) and low infection-related risk (n = 63) groups based on the model's best threshold of 0.357. This stratification yielded a recall of 0.839, a specificity of 0.716, and a negative predictive value of 0.841. Using the win ratio method to analyze the hierarchical composite endpoint comprising all-cause death, organ failure, sepsis, new-onset acute decompensation, and SIRS, the high-risk group had more wins than the low-risk group (50.4% *vs*. 24.9%, win ratio: 2.03 (95% CI: 1.21–3.39), $P = 0.007$, Fig. 6). This result was primarily driven by death, organ failure, and sepsis, indicating that patients in the high-risk group had worse 90-day outcomes than those in the low-risk group. Reordering of the hierarchical components did not affect the robustness of the analysis (Supplementary Table 19).

Non-ACLF patients in the validation set were stratified into high infection-related risk (n = 83) and low infection-related risk (n = 174) groups based on the model's best threshold of 0.378. This stratification yielded a recall of 0.818, a specificity of 0.772, and a negative predictive value of 0.954. The high-risk group also had worse 90-day outcomes than the low-risk group (win ratio: 7.13 (95% CI: 3.66–13.89), $P < 0.001$, Supplementary Table 20).

Model interpretation

SHAP analysis identified thyroxine, followed by 2-isopropylmalate, pipecolate, 1-linoleoyl-GPE (18:2), and S1P, as the top predictors in the ACLF infection model (Supplementary Fig. 10A). In the non-ACLF infection model, 3-phenylpropionate, ribitol, and 1-linoleoyl-GPC (18:2) were the top three contributors (Supplementary Fig. 10B).

The SHAP waterfall plots illustrated how individual predictions were generated. For an ACLF patient who was correctly diagnosed with infection, decreased 1-linoleoyl-GPE (18:2), S1P, and thyroxine, along with increased pipecolate, pushed the prediction toward infection, whereas 2-isopropylmalate pushed it away from infection (Supplementary Fig. 10C). In non-ACLF, infection prediction was driven by positive contributions from orotate, 1-carboxyethylphenylalanine, S1P, 1-linoleoyl-GPC (18:2), and 3-phenylpropionate, while ribitol contributed negatively (Supplementary Fig. 10D).

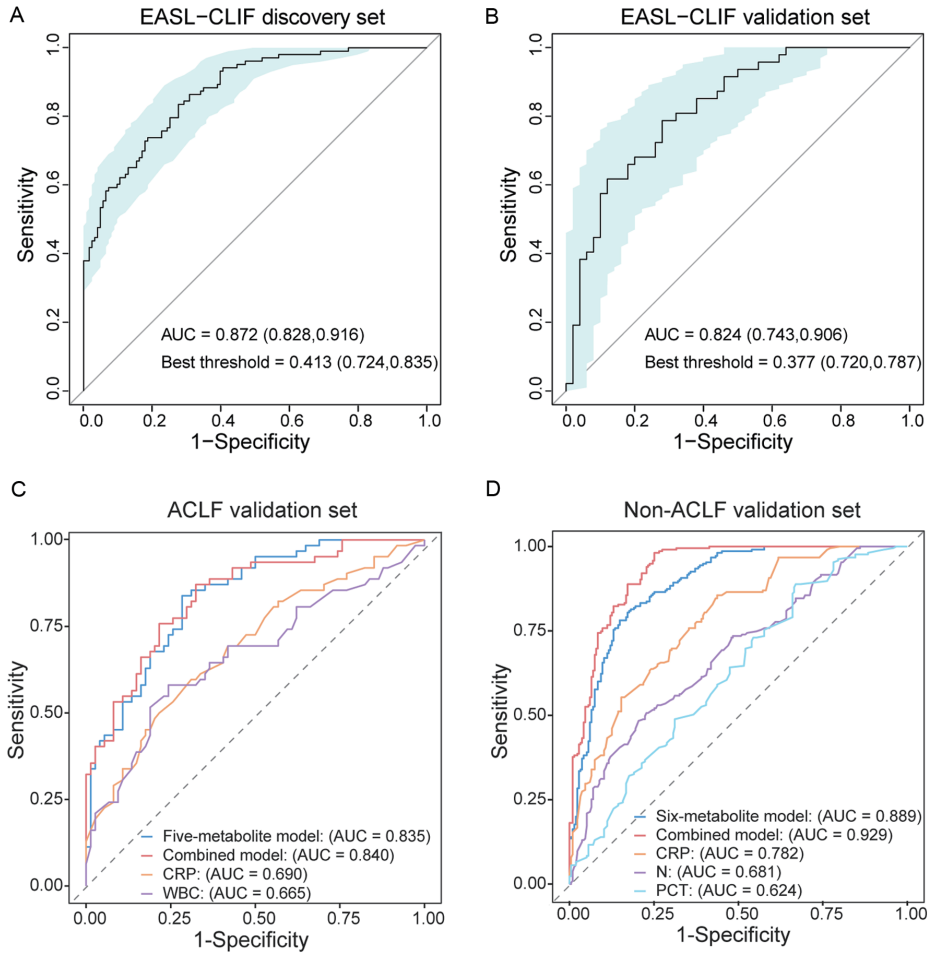

Fig. 5. Performance of the five-metabolite model under the EASL-CLIF ACLF criteria and comparison of models with conventional markers under the COSSH criteria. (A, B) Performance of the five-metabolite model according to the EASL-CLIF ACLF criteria in (A) the discovery set and (B) the validation set. (C) Comparison of ROC curves: five-metabolite model, five-metabolite model + CRP (combined model), CRP, and WBC in ACLF. (D) Comparison of ROC curves: six-metabolite model, six-metabolite model + CRP (combined model), CRP, N, and PCT in non-ACLF. ACLF, acute-on-chronic liver failure; AUC, area under the curve; COSSH, the Chinese Group on the Study of Severe Hepatitis B; CRP, C-reactive protein; EASL-CLIF, European Association for the Study of the Liver - Chronic Liver Failure; N, neutrophil count; PCT, procalcitonin; ROC, receiver operating characteristic; WBC, white blood cell count.

SHAP dependence plots showed how the model output varied with the log2-transformed relative abundance of metabolites. In ACLF, log2 (relative abundance) thresholds of thyroxine < 18.66, S1P < 18.71, 1-linoleoyl-GPE (18:2) < 23.06, pipecolate > 28.05, and 2-isopropylmalate > 19.58 pushed classification toward infection (Supplementary Fig. 10E). In non-ACLF, thresholds associated with infection were S1P < 19.40, 3-phenylpropionate < 19.14, 1-linoleoyl-GPC (18:2) < 26.20, orotate > 21.39, ribitol > 19.33, and 1-carboxyethylphenylalanine > 19.60 (Supplementary Fig. 10F).

Discussion

This study delineated plasma metabolic alterations associated with bacterial infection in patients with AoCLD and identified key diagnostic biomarkers through metabolomics profiling. ACLF and non-ACLF patients have distinct plasma metabolomic profiles.[16] To precisely address the different clinical needs of this heterogeneous population, we developed a disease-stage-specific early diagnostic framework. The framework outperformed conventional infection indicators (CRP, WBC, and PCT) and the best composite clinical model. As HBV patients comprised the highest proportion of our cohort, we initially used the COSSH-ACLF criteria to define ACLF and then used the EASL-CLIF ACLF criteria to validate these biomarkers.[17]

Consistent with previous studies, the five metabolites in our model were associated with bacterial infection in ACLF. Thyroxine regulates innate and adaptive immunity, and its serum concentration decreases during severe infections.[22] Low thyroxine levels are predictors of hepatic encephalopathy in patients with cirrhosis.[26] 2-Isopropylmalate is a key intermediate in bacterial biosynthesis of leucine. We found that its levels correlated with CRP and NLR. Pipecolate, a catabolite of lysine, exhibits elevated levels associated with infection and liver injury.[23] 1-linoleoyl-GPE (18:2) is a lysophosphatidylethanolamine (LysoPE). LysoPEs can support gut homeostasis and barrier function and possess antimicrobial activity.[27] S1P is a lipid signaling molecule linked to inflammation. A previous study found significantly reduced serum S1P levels in sepsis, consistent with our findings.[21] In addition, we observed significant correlations between S1P levels and markers of inflammation and immunity, including WBC, CRP, neutrophils, and albumin.

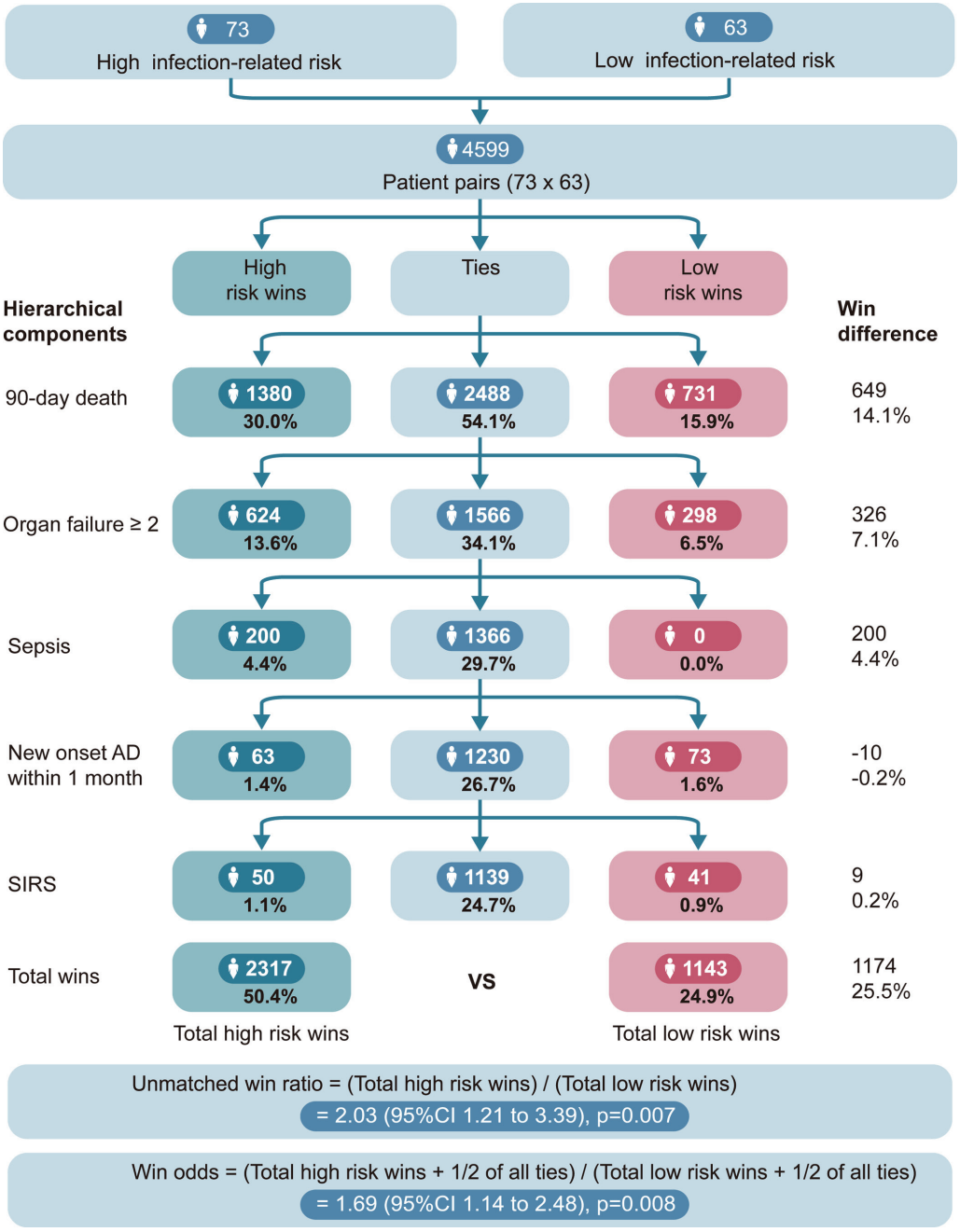

Fig. 6. Win ratio diagram for the infection-related hierarchical composite endpoint in ACLF. The endpoints were prioritized for evaluation in the following order of clinical importance: 90-day death, organ failure, sepsis, new-onset AD, and SIRS. For each component of the hierarchical composite endpoint, patient pairs were compared and classified as: wins in the high-risk group, ties, or wins in the low-risk group. ACLF, acute-on-chronic liver failure; AD, acute decompensation; SIRS, systemic inflammatory response syndrome.

The 6-metabolite non-ACLF model shares S1P with the ACLF model. The other five metabolites reflect the interplay between bacterial infection and host antimicrobial defense. 1-linoleoyl-GPC (18:2) is a lysophosphatidylcholine (LysoPC) produced by phospholipase-mediated cleavage of phosphatidylcholine, which has been shown to prevent microbial infection and treat sepsis.[28] Consistently, we observed significant downregulation of various LysoPCs in infected patients. 3-phenylpropionate promotes intestinal epithelial barrier formation and exhibits antimicrobial activity.[29] Ribitol is a Gram-positive bacterial cell wall component. Increased orotate reflects pyrimidine pathway perturbation due to bacterial metabolism.[24] 1-carboxyethylphenylalanine, a phenylalanine derivative, indicates elevated oxidative stress.[30]

The panel of metabolites used in the diagnostic models for bacterial infection differs between ACLF and non-ACLF patients. This suggests that liver function status may influence the diagnostic performance of these markers. A possible explanation is that severe liver impairment compromises biosynthetic and immune functions. The model performance

showed mild differences among ACLF grades but remained robust overall (AUCs: 0.824–0.859 in the validation set). This indicates its potential applicability across ACLF populations of varying severity. Exploring the heterogeneity of host metabolic responses to bacterial infection across liver function statuses and extrahepatic organ failure conditions is a promising research direction. Metabolomic profiles may also differ by infection type or pathogen. In our cohort, metabolic differences between the two most common infection types (pulmonary infection and SBP) were limited (Supplementary Tables 21 and 22). A previous study identified species-specific metabolic signatures of *Acinetobacter baumannii* and *Klebsiella pneumoniae* infections in ACLF, indicating that metabolomic profiles may vary by pathogen.[31] However, whether pathogens directly affect metabolism remains unclear. In the future, models can be developed for populations with specific infection types or pathogens, and animal models can be used to explore their impact on metabolism. Class imbalance can bias models toward the majority class. To avoid overfitting and noise, we did not apply sampling techniques to the ACLF group, which was relatively balanced (prevalence: 0.439). In contrast, the non-ACLF group was imbalanced (prevalence: 0.153), so we applied SMOTE only to its discovery set.[32]

When analyzing composite endpoints for prognosis, we usually focus on multiple clinical outcomes and prioritize more severe events. Traditional approaches often treat all clinical events as equally important and focus only on the first-occurring endpoint. These methods are inconsistent with real-world clinical scenarios. For example, subsequent fatal events (death) may be overlooked when patients experience non-fatal prognostic events (e.g., sepsis). We used the win ratio method to emphasize differences in the clinical importance of infection-related outcomes.[20] All-cause death was designated as the most important endpoint. To mitigate the impact of tied events, we calculated win odds; the results also supported our conclusions.

This study has several advantages. First, it was based on a large-scale, prospective multicenter cohort that is representative of the Chinese AoCLD population, in which HBV was the predominant etiology. Second, the ACLF model showed consistent diagnostic performance when applied according to the two major ACLF criteria. Third, it accounted for plasma metabolome heterogeneity during disease progression and identified novel metabolic biomarkers for bacterial infection in ACLF. Finally, risk stratification based on baseline metabolic levels was aligned with 90-day outcomes, demonstrating its potential for prognostic management.

This study also has several limitations. First, as a proof-of-concept investigation, it provided potential biomarkers for clinical practice; however, the models were not externally validated in an independent cohort, which may limit the generalizability of our findings across different populations and clinical settings. Second, our model performed well in the HBV-predominant ACLF population but requires further validation in cohorts where other etiologies, such as alcohol-related liver disease, predominate. Third, future studies should validate how metabolic biomarkers relate to the progression of ACLF or infection through interventional animal studies or clinical trials. Finally, as the definition of ACLF is not yet uniform, these findings require further external validation across multiple ACLF definitions in more recent cohorts.

Given a 90-day mortality of 45.45% in ACLF patients with bacterial infection, early and accurate diagnosis is critical. Our model demonstrated moderate to high discriminatory ability and provided a complementary tool that outperformed conventional indicators, including CRP, WBC, and the best composite clinical model. Using a threshold of 0.357, patients classified as high-risk by the model had significantly worse 90-day outcomes than those classified as low-risk, indicating the early warning value of this stratification approach. Early antimicrobial treatment in high-risk patients identified by these biomarkers may improve survival and reduce unnecessary empirical antibiotic use. Building on our prior work in translating metabolic biomarkers into a practical test,[16] future efforts will focus on developing rapid diagnostic tests based on targeted quantitative assays and integrating them into a clinical decision-support system for individualized management.

Conclusions

This study delineated the metabolic landscape of AoCLD associated with bacterial infection. Based on novel metabolite biomarkers, we developed diagnostic models for bacterial infection tailored to the ACLF disease spectrum. These models outperformed conventional indicators. A risk stratification strategy based on baseline metabolic perturbations can indicate the risk of 90-day outcomes. Plasma metabolic biomarkers in these models may serve as reference indicators to enhance precise diagnosis and personalized management in patients with AoCLD.

Supporting information

Supplementary material for this article is available at https://doi.org/10.14218/JCTH.2026.00384.

Funding

This work was supported by the Prevention and Control of Emerging and Major Infectious Diseases-National Science and Technology Major Project (Grant No. 2026ZD0191220), the National Natural Science Foundation of China (Grant No. 82300720), and the Hubei Provincial Natural Science Foundation Project (Grant No. 2025AFA036).

Conflict of interest

LG is an employee of Shanghai Gan Ning Medical Technology Inc. YS and YZ has been an Editorial Board Member of *Journal of Clinical and Translational Hepatology* since 2020. The other authors have no conflict of interests related to this publication.

Author contributions

Conceptualization and data curation (XZ, LG, HL, YH, GD, XW, BL, ZM, YZ, YG, ZQ, FL, XL, YS, JS), supervision (XZ, HL, YH, GD, XW, BL, ZM, YZ, YG, ZQ, FL, XL), methodology (XY, XZ, LG), project administration (XZ, HL), visualization (XY, HJ), analysis of data (XY, LG, XZ), investigation (XY, JL, SL), and writing – review & editing (XZ, LG, XY). All authors have approved the final manuscript.

Ethical statement

This study was approved by the Ethics Committee of Renji Hospital, Shanghai Jiao Tong University School of Medicine, Shanghai, China (2014-148K and 2016-142K). All patients provided written informed consent to participate in the study. The research was conducted in accordance with the Declaration of Helsinki (as revised in 2024) and the Declaration of Istanbul. This study was registered at ClinicalTrials.gov (NCT02457637, NCT03641872).

Data sharing statement

Data used in this study can be obtained from the corresponding authors upon reasonable request.

References

[1] Bernal W, Jalan R, Quaglia A, Simpson K, Wendon J, Burroughs A. Acute-on-chronic liver failure. Lancet 2015;386(10003):1576–1587. doi:10.1016/S0140-6736(15)00309-8, PMID:26423181.

[2] Hernaez R, Kramer JR, Liu Y, Tansel A, Natarajan Y, Hussain KB, *et al*. Prevalence and short-term mortality of acute-on-chronic liver failure: A national cohort study from the USA. J Hepatol 2019;70(4):639–647. doi:10.1016/j.jhep.2018.12.018, PMID:30590100.

[3] Mezzano G, Juanola A, Cardenas A, Mezey E, Hamilton JP, Pose E, *et al*. Global burden of disease: acute-on-chronic liver failure, a systematic review and meta-analysis. Gut 2022;71(1):148–155. doi:10.1136/gutjnl-2020-322161, PMID:33436495.

[4] Wong F, Piano S, Singh V, Bartoletti M, Maiwall R, Alessandria C, *et al*. Clinical features and evolution of bacterial infection-related acute-on-chronic liver failure. J Hepatol 2021;74(2):330–339. doi:10.1016/j.jhep.2020.07.046, PMID:32781201.

[5] Dionigi E, Garcovich M, Borzio M, Leandro G, Majumdar A, Tsami A, *et al*. Bacterial Infections Change Natural History of Cirrhosis Irrespective of Liver Disease Severity. Am J Gastroenterol 2017;112(4):588–596. doi:10.1038/ajg.2017.19, PMID:28220780.

[6] Bernsmeier C, Triantafyllou E, Brenig R, Lebosse FJ, Singanayagam A, Patel VC, *et al*. CD14(+) CD15(-) HLA-DR(-) myeloid-derived suppressor cells impair antimicrobial responses in patients with acute-on-chronic liver failure. Gut 2018;67(6):1155–1167. doi:10.1136/gutjnl-2017-314184, PMID:28592438.

[7] Wasmuth HE, Kunz D, Yagmur E, Timmer-Stranghöner A, Vidacek D, Siewert E, *et al*. Patients with acute on chronic liver failure display "sepsis-like" immune paralysis. J Hepatol 2005;42(2):195–201. doi:10.1016/j.jhep.2004.10.019, PMID:15664244.

[8] Chen T, Chen G, Wang G, Treeprasertsuk S, Lesmana CRA, Lin HC, *et al*. Expert consensus on the diagnosis and treatment of end-stage liver disease complicated by infections. Hepatol Int 2024;18(3):817–832. doi:10.1007/s12072-023-10637-3, PMID:38460060.

[9] Lin S, Yan YY, Wu YL, Wang MF, Zhu YY, Wang XZ. Development of a novel score for the diagnosis of bacterial infection in patients with acute-on-chronic liver failure. World J Gastroenterol 2020;26(32):4857–4865. doi:10.3748/wjg.v26.i32.4857, PMID:32921962.

[10] Izumi S, Hughes RD, Langley PG, Pernambuco JR, Williams R. Extent of the acute phase response in fulminant hepatic failure. Gut 1994;35(7):982–986. doi:10.1136/gut.35.7.982, PMID:8063228.

[11] Leticia Fernandez-Carballo B, Escadafal C, MacLean E, Kapasi AJ, Dittrich S. Distinguishing bacterial versus non-bacterial causes of febrile illness - A systematic review of host biomarkers. J Infect 2021;82(4):1–10. doi:10.1016/j.jinf.2021.01.028, PMID:33610683.

[12] Asrani SK, Simonetto DA, Kamath PS. Acute-on-Chronic Liver Failure. Clin Gastroenterol Hepatol 2015;13(12):2128–2139. doi:10.1016/j.cgh.2015.07.008, PMID:26188138.

[13] Trebicka J, Fernandez J, Papp M, Caraceni P, Laleman W, Gambino C, *et al*. The PREDICT study uncovers three clinical courses of acutely decompensated cirrhosis that have distinct pathophysiology. J Hepatol 2020;73(4):842–854. doi:10.1016/j.jhep.2020.06.013, PMID:32673741.

[14] Wu T, Li J, Shao L, Xin J, Jiang L, Zhou Q, *et al*. Development of diagnostic criteria and a prognostic score for hepatitis B virus-related acute-on-chronic liver failure. Gut 2018;67(12):2181–2191. doi:10.1136/gutjnl-2017-314641, PMID:28928275.

[15] Garg P, Verma N, Valsan A, Sarohi V, Basak T, Gupta T, *et al*. Proteomics-guided Biomarker Discovery, Validation, and Pathway Perturbation in Infection-related Acute Decompensation of Cirrhosis. Clin Gastroenterol Hepatol 2026;24(2):407–420.e39. doi:10.1016/j.cgh.2025.01.005, PMID:39924007.

[16] Zhang Y, Tan W, Wang X, Zheng X, Huang Y, Li B, *et al*. Metabolic biomarkers significantly enhance the prediction of HBV-related ACLF occurrence and outcomes. J Hepatol 2023;79(5):1159–1171. doi:10.1016/j.jhep.2023.07.011, PMID:37517452.

[17] European Association for the Study of the Liver. EASL Clinical Practice Guidelines on acute-on-chronic liver failure. J Hepatol 2023;79(2):461–491. doi:10.1016/j.jhep.2023.04.021, PMID:37364789.

[18] Fernández J, Acevedo J, Wiest R, Gustot T, Amoros A, Deulofeu C, *et al*. Bacterial and fungal infections in acute-on-chronic liver failure: prevalence, characteristics and impact on prognosis. Gut 2018;67(10):1870–1880. doi:10.1136/gutjnl-2017-314240, PMID:28847867.

[19] Bajaj JS, O'Leary JG, Reddy KR, Wong F, Biggins SW, Patton H, *et al*. Survival in infection-related acute-on-chronic liver failure is defined by extrahepatic organ failures. Hepatology 2014;60(1):250–256. doi:10.1002/hep.27077, PMID:24677131.

[20] Pocock SJ, Ariti CA, Collier TJ, Wang D. The win ratio: a new approach to the analysis of composite endpoints in clinical trials based on clinical priorities. Eur Heart J 2012;33(2):176–182. doi:10.1093/eurheartj/ehr352, PMID:21900289.

[21] Wang B, Wu X, Cheng J, Ye J, Zhu H, Liu X. Regulatory role of S1P and its receptors in sepsis-induced liver injury. Front Immunol 2025;16:1489015. doi:10.3389/fimmu.2025.1489015, PMID:39935473.

[22] Wenzek C, Boelen A, Westendorf AM, Engel DR, Moeller LC, Führer D. The interplay of thyroid hormones and the immune system - where we stand and why we need to know about it. Eur J Endocrinol 2022;186(5):R65–R77. doi:10.1530/EJE-21-1171, PMID:35175936.

[23] Kawasaki H, Hori T, Nakajima M, Takeshita K. Plasma levels of pipecolic acid in patients with chronic liver disease. Hepatology 1988;8(2):286–289. doi:10.1002/hep.1840080216, PMID:3356409.

[24] Garavito MF, Narváez-Ortiz HY, Zimmermann BH. Pyrimidine Metabolism: Dynamic and Versatile Pathways in Pathogens and Cellular Development. J Genet Genomics 2015;42(5):195–205. doi:10.1016/j.jgg.2015.04.004, PMID:26059768.

[25] Ma S, Yang B, Sun Y, Wang X, Guo H, Liu R, *et al*. Salmonella exploits host- and bacterial-derived β-alanine for replication inside host macrophages. Elife 2025;13:RP103714. doi:10.7554/eLife.103714, PMID:40536105.

[26] Bajaj JS, Tandon P, O'Leary JG, Reddy KR, Garcia-Tsao G, Thuluvath P, *et al*. Admission Serum Metabolites and Thyroxine Predict Advanced Hepatic Encephalopathy in a Multicenter Inpatient Cirrhosis Cohort. Clin Gastroenterol Hepatol 2023;21(4):1031–1040.e3. doi:10.1016/j.cgh.2022.03.046, PMID:35436625.

[27] Zou D, Pei J, Lan J, Sang H, Chen H, Yuan H, *et al*. A SNP of bacterial blc disturbs gut lysophospholipid homeostasis and induces inflammation through epithelial barrier disruption. EBioMedicine 2020;52:102652. doi:10.1016/j.ebiom.2020.102652, PMID:32058942.

[28] Yan JJ, Jung JS, Lee JE, Lee J, Huh SO, Kim HS, *et al*. Therapeutic effects of lysophosphatidylcholine in experimental sepsis. Nat Med 2004;10(2):161–167. doi:10.1038/nm989, PMID:14716308.

[29] Hu J, Chen J, Xu X, Hou Q, Ren J, Yan X. Gut microbiota-derived 3-phenylpropionic acid promotes intestinal epithelial barrier function via AhR signaling. Microbiome 2023;11(1):102. doi:10.1186/s40168-023-01551-9, PMID:37158970.

[30] Depommier C, Everard A, Druart C, Maiter D, Thissen JP, Loumaye A, *et al*. Serum metabolite profiling yields insights into health promoting effect of A. muciniphila in human volunteers with a metabolic syndrome. Gut Microbes 2021;13(1):1994270. doi:10.1080/19490976.2021.1994270, PMID:34812127.

[31] Cadoli C, Arif S, Ballhorn W, Brieger A, Brol MJ, Castelli F, *et al*. Metabolic Signatures of Acinetobacter baumannii and Klebsiella pneumoniae Infections in Acute-on-chronic Liver Failure. Cell Mol Gastroenterol Hepatol 2026;20(4):101707. doi:10.1016/j.jcmgh.2025.101707, PMID:41389877.

[32] Megahed FM, Chen YJ, Megahed A, Ong Y, Altman N, Krzywinski M. The class imbalance problem. Nat Methods 2021;18(11):1270–1272. doi:10.1038/s41592-021-01302-4, PMID:34654918.